THE JOURNAL OF PHYSICAL CHEMISTRY B

Article

pubs.acs.org/JPCB

# Molecular Dynamics Simulation of the Aggregation Patterns in Aqueous Solutions of Bile Salts at Physiological Conditions

Fatmegyul Mustan,[†] Anela Ivanova,[*,‡] Galia Madjarova,[‡] Slavka Tcholakova,[†] and Nikolai Denkov[†]

[†]Department of Chemical and Pharmaceutical Engineering, and [‡]Department of Physical Chemistry, Faculty of Chemistry and Pharmacy, University of Sofia, 1 James Bourchier Avenue, 1164 Sofia, Bulgaria

Supporting Information

**ABSTRACT:** Classical molecular dynamics simulations are employed to monitor the aggregation behavior of six bile salts (nonconjugated and glycine- and taurine-conjugated sodium cholate and sodium deoxycholate) with concentration of 10 mM in aqueous solution in the presence of 120 mM NaCl. There are 150 ns trajectories generated to characterize the systems. The largest stable aggregates are analyzed to determine their shape, size, and stabilizing forces. It is found that the aggregation is a hierarchical process and that its kinetics depends both on the number of hydroxyl groups in the steroid part of the molecules and on the type of conjugation. The micelles of all salts are similar in shape—deformed spheres or ellipsoids, which are stabilized by hydrophobic forces, acting between the steroid rings. The differences in the aggregation kinetics of the various conjugates are rationalized by the affinity for hydrogen bond formation for the glycine-modified salts or by the longer time needed to achieve optimum packing for the tauro derivatives. Evidence is provided for the hypothesis from the literature that the entirely hydrophobic core of all aggregates and the enhanced dynamics of the molecules therein should be among the prerequisites for their pronounced solubilization capacity for hydrophobic substances *in vivo*.

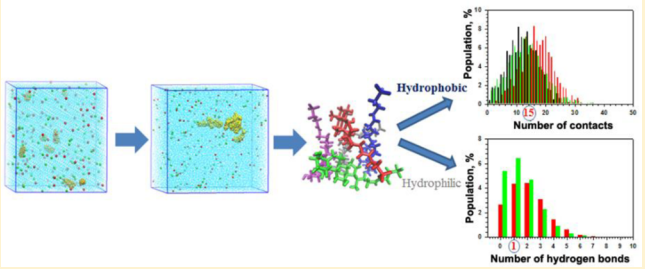


## INTRODUCTION

Bile acids (BAs) are bioactive compounds synthesized from cholesterol in the liver. Most of them, bound to glycine or taurine residues, are ionic along the gastrointestinal tract. One of the most important BA specifics is the formation of aggregates, which solubilize the hydrophobic products of the enzymatic hydrolysis of triglycerides upon digestion in the gastrointestinal tract and facilitate their metabolism. Due to their vast practical significance BA aggregates have been intensively studied experimentally. The most frequently used methods for determination of the aggregates' size are laser light scattering, small-angle neutron scattering, proton NMR, and cryogenic transmission electron microscopy (cryo-TEM).[1,2]

Small and co-workers[3] investigated the aggregation numbers ($N_{agg}$) of bile salts (BS) by ultracentrifugation and by laser light scattering. They discovered that all trihydroxy bile salts form very small micelles with $N_{agg}$ < 10, which are resistant to changes in counterion concentration or temperature. Dihydroxy BS formed small micelles at low concentration (around the critical micelle concentration, CMC) and large micelles ($N_{agg}$ = 12−100) at higher concentration (well above the CMC). A temperature increase resulted in a significant decrease in the micelle aggregation number. It was shown that pH had mild effect on $N_{agg}$ of the trihydroxy derivatives while the size of the dihydroxy aggregates increased upon pH lowering down to values around p$K_a$ of the bile acids.

A convention exists in the literature to denote the smaller micelles as *primary* and the larger ones as *secondary*.[3] It is believed that primary micelles typically assemble via hydrophobic forces,[4] and their aggregation numbers vary in the range 2−9 molecules. Secondary micelles are formed by hydrogen bonding of the primary ones, and their $N_{agg}$ values span a much wider range. According to Small and co-workers,[3] only dihydroxy BS can yield secondary micelles whereas the trihydroxy ones assemble predominantly into primary micelles.

The aggregation of taurine-conjugated cholate (TCH, trihydroxy BA) and deoxycholate (TDCH, dihydroxy BA) was studied experimentally to determine $N_{agg}$ and the radius of the micelles. The latter was measured by ultracentrifugation, gel filtration, and free diffusion.[5−7] For TDCH with concentrations slightly above CMC in aqueous solution with 150 mM NaCl at 20 °C, $N_{agg}$ was 18, which indicated the formation of secondary micelles. Their apparent radius was between 2 and 2.4 nm. For TCH in the same concentration range and at identical ionic strength but at 37 °C, $N_{agg}$ was 5, and the radius was ca. 1 nm.

More recent reports of various authors[8−14] confirmed the exceptionally small aggregation number of bile salts $2 \leq N_{agg} \leq 15$ (in aqueous solution with 150 mM NaCl, pH 7, room temperature). It was shown that $N_{agg}$ depends on the type of the surfactant, nonconjugated or glycine- or taurine-conjugated, as well as on the number, orientation, and position of hydroxyl groups in the steroid ring. It was established also that

**Received:** July 22, 2015
**Revised:** November 16, 2015
**Published:** November 25, 2015





DOI: 10.1021/acs.jpcb.5b07063
J. Phys. Chem. B 2015, 119, 15631−15643

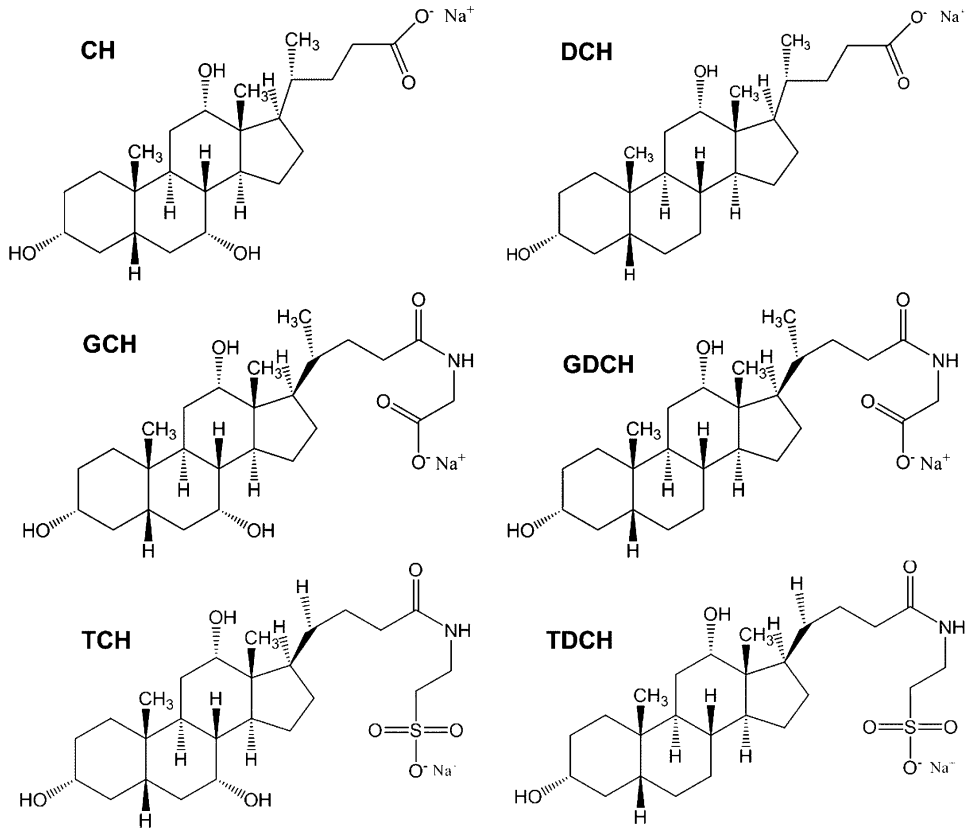


**Figure 1.** Chemical structures of the bile salts most abundant in the human organism, which are studied in the present work. The abbreviations of each molecule used throughout the text are denoted.

deoxycholates had larger $N_{agg}$ than cholates and that tauro-conjugates formed smaller micelles than glyco-derivatives. None of these studies, however, reported exact structures and sizes of the micelles. It was stated only that the aggregates were very dynamic and flexible.

There are also theoretical communications in the literature, addressing the aggregation process of BS mostly by molecular dynamics (MD) simulations. Partay et al.[15] studied the behavior of aqueous solutions of sodium cholate (CH) and deoxycholate (DCH) at three concentrations: 30, 90, and 300 mM. Parameters based on the classical force field GROMOS87 were used for the bile salts and for the ions, while the model SPC/E was employed for water. All systems were simulated at room temperature. It was found that the two salts formed only oligomers at the lowest concentration, which is closest to the physiological concentration, determined *in vivo* in humans. Those of DCH were stabilized by hydrophobic attraction forces between the steroid rings. For CH aggregates, intermolecular hydrogen bonding was reported in addition to the hydrophobic interactions. $N_{agg}$ for cholate was 4.5 and for deoxycholate −4.1, the largest aggregates of the two BS being pentamers and hexamers, respectively. At the highest studied concentration, the molecules formed secondary micelles, which were stabilized by hydrophobic interactions and hydrogen bonds. An aggregate size of 30−40 molecules was reported. It was concluded that the secondary micelles of DCH were formed by hydrogen bonding of smaller hydrophobically stabilized primary micelles. On the contrary, the secondary micelles of CH resulted from hydrophobic attraction of hydrophobically or H-bonded small clusters.

The same authors showed[16] that the molecular structure of bile salts, which differs considerably from that of conventional surfactants, is the reason for obtaining micelles of various shapes: ellipsoid or rod-like. It was observed that the preferred molecular orientation within the micelles is with parallel steroid parts of the neighboring molecules. Spherical primary micelles were reported for DCH while CH assembled into disc-like or ellipsoid shapes.

Similar aggregate shapes were observed by Warren et al.[17] who simulated by MD the aggregation of six bile salts: cholate, glycocholate (GCH), taurocholate, glycochenodeoxycholate, glycodeoxycholate (GDCH), and glycolithocholate in aqueous solution with concentration of ∼100 mM. $N_{agg}$ varied between 8 and 17. The obtained results showed that the shape of the micelles ranges from deformed sphere to elongated structures, in which the molecules face their steroid rings. The authors concluded that intermolecular hydrogen bonds were the main factor influencing the size, structure, and dynamics of the micelles.

Verde et al.[18] performed coarse-grained MD simulations of different bile salts in implicit solvent and found small micelles with close to spherical shape and larger, more elongated ones for two types of BS (with two and three hydroxyl groups). The analysis of micelle formation of these two molecules and of a hypothetical derivative without hydroxyl groups revealed that the trihydroxy modification formed smaller micelles than the dihydroxy one at a given concentration, while the hypothetical molecule gave the largest aggregates. Since hydrogen bonds were not taken into account in these simulations, while micelles formed regardless of that, the authors assumed that hydrogen bonding was not essential for formation of the small micelles



DOI: 10.1021/acs.jpcb.5b07063
J. Phys. Chem. B 2015, 119, 15631−15643

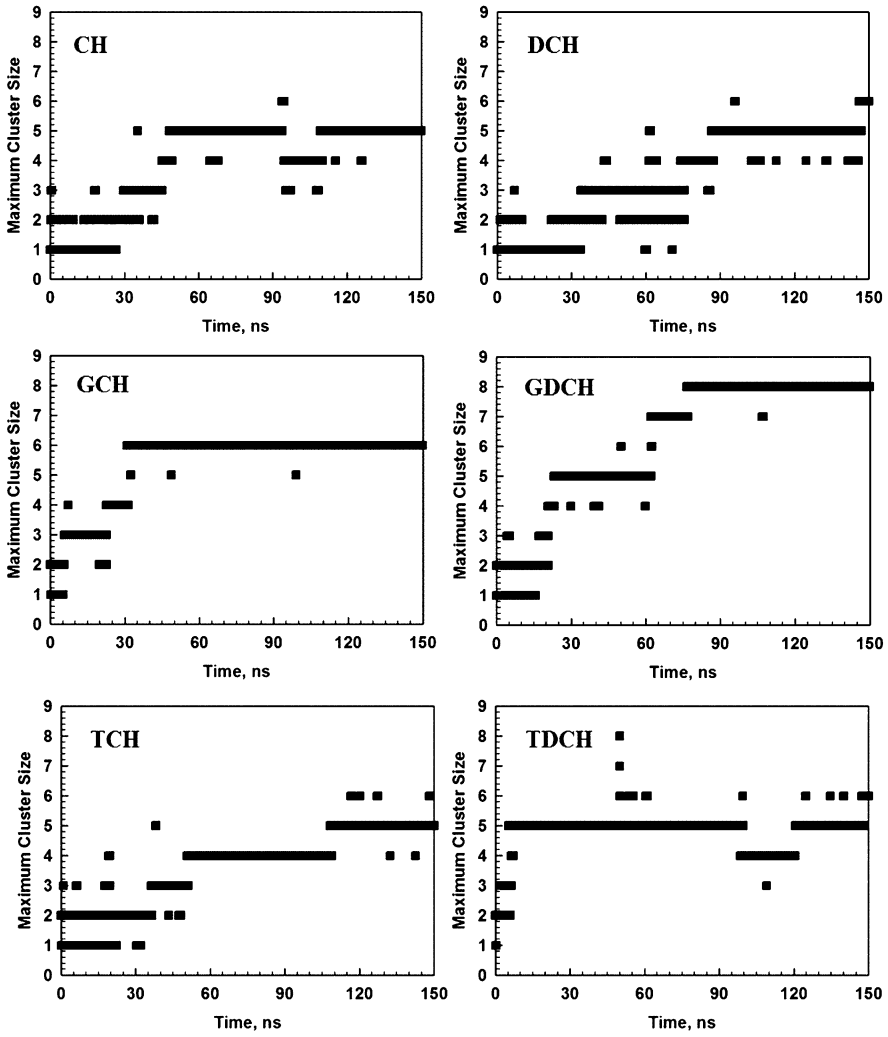


**Figure 2.** Evolution of the maximum cluster size of the six studied systems during the MD simulations.

and that they were stabilized by hydrophobic forces. The authors suggested also that the profound dynamics of the molecules within the micelles had physiological relevance for the formation of mixed micelles with lipophilic substances from the gastrointestinal tract.

A survey of the literature showed no theoretical reports on the kinetics of bile salt aggregation at concentrations close to the physiological conditions *in vivo*, i.e., about 10 mM, in spite of the known fact that the aggregation of these compounds depends strongly on their bulk concentration.[3] The above synopsis also indicates that there is no unified opinion on the nature of the driving force for aggregation of BS in aqueous solution. Hence, the aims of the present study are 2-fold: (1) to monitor the kinetics of aggregation of 6 bile salts (non-conjugated and glycine- and taurine-conjugated cholate and deoxycholate, respectively; see Figure 1) in aqueous solution with bile concentration of 10 mM in the presence of 120 mM NaCl at 37 °C and to elucidate the interactions influencing the rate of aggregates formation, (2) to analyze the intermolecular forces acting within the most stable aggregates and defining their shape and size, and how these interactions are affected by the conjugation in the hydrophilic head of the molecules and by the number of hydroxyl groups in the steroid fragment.

The ultimate goal of the study is to reveal the factors defining the solubilization capacity of BA micelles for hydrophobic substances such as cholesterol, products of triglycerides hydrolysis, and pharmaceutics, at conditions mimicking those in the human gastrointestinal tract. The present work can be regarded as the first step in this direction.

## MOLECULAR MODELS AND COMPUTATIONAL PROTOCOL

The setup of the virtual experiment was aimed to reproduce as much as possible, within the limitations of the method, real experimental conditions[19] which mimic the situation *in vivo*. The concentration of bile salts in the aqueous solution model is 10 mM, and that of NaCl is 120 mM. These concentrations correspond to 8 molecules of bile anions neutralized by 8 sodium cations in each simulation box with edge length 11 nm. All boxes are cubic, and each of them contains also 112 $Na^+$, 112 $Cl^-$, and ca. 43 600 water molecules, which result in total volume of each model system of $1.331 \times 10^{-24}$ $m^3$ (see Figure S1 of the Supporting Information for illustration). Periodic boundary conditions are applied in the three directions throughout the simulations to model continuous solutions. In the initial configurations all ions are placed randomly in the simulation boxes and are then left to self-assemble during the MD runs.

The force field AMBER99[20,21] is used for all ions, while the model TIP3P[22] is employed for the water molecules. Since



DOI: 10.1021/acs.jpcb.5b07063
J. Phys. Chem. B 2015, 119, 15631−15643

AMBER does not contain parameters for the sulfate fragment of taurine, the necessary values are adopted from Gaff (Table S1).[23] The atomic charges of the BS needed to calculate the electrostatic contribution to the energy are derived by applying the RESP procedure[24,25] where the charges are fit to the quantum mechanical electrostatic potential of each molecule, generated at the HF/6-31G* level for geometries of the molecules optimized with the DFT functional B3LYP[26−29] and basis set 6-31G*[30] within the program package Gaussian09.[31] The final RESP charges (Tables S2.1 and S2.2 and Figure S2 in the Supporting Information) are averaged over the most stable conformers of each molecule. The atom types of all atoms are also provided in the Supporting Information (Table S3).

The following computational procedure is applied to all studied systems: energy minimization of the initial configuration, heating to 310 K, relaxation for 0.5 ns, and production runs with length 150 ns. The time step is 2 fs. All MD simulations are done in NVT ensemble to comply with the desired concentration. Constant temperature is maintained with the Berendsen thermostat[32] with coupling constant of 0.1 ps. The algorithm leapfrog is used to integrate the equations of motion. The lengths of all hydrogen-containing bonds are fixed with SETTLE[33] (for the water molecules) and LINCS[34] (for the bile salts). The Lennard-Jones potential is truncated at 10 Å with a switch function turned on at 8 Å. Electrostatic interactions are evaluated in the monopole approximation with the method PME;[35−37] the cutoff for the direct part of the sum is 12 Å with a switch function initiated at 10 Å. Equilibration of the systems is verified by monitoring the evolution of the total energy and temperature, and of the temperatures of the separate components. The RMSD variation of the BS atomic coordinates with time is selected as a structural criterion. All these parameters fluctuate around constant average values during the production runs, which confirms that thermodynamic equilibrium has been attained. However, the bile salt aggregates are analyzed only after the self-assembly process of each system has reached the stationary state (see Figure 2 and discussion in the text).

The production trajectories are subject to statistical analysis including snapshots separated by 1 ps. The entire production stage of 150 ns is used only to monitor the kinetics of aggregation. The properties of the most stable aggregates (see below) are obtained by processing only the part of the MD trajectories where they exist (Table 1). The program package GROMACS 4.5.2[38] is used for all simulations and for analysis. VMD[39] is employed for visualization of the trajectories.

**Table 1. Summarized Data for Calculated and Experimental Aggregation Numbers ($N_{agg}$'s), Moments of Formation ($\tau_f$), and Relative Population[a] of the Most Stable Aggregates of the Six Studied Bile Salts**

| molecule | $N_{agg}^{calc}$ | $N_{agg}^{exp}$ | $\tau_f$, ns | population, % |
|---|---|---|---|---|
| CH | 5 | 4.8 | 48.3 | 57.8 |
| DCH | 5 | 13.3 | 86.5 | 39.7 |
| GCH | 6 | 5.6 | 31.3 | 78.9 |
| GDCH | 8 | 16.2 | 77.0 | 48.7 |
| TCH | 5 | 4.5 | 108.9 | 27.4 |
| TDCH | 5 | 18.0 | 6.4 | 79.0 |

[a]Obtained as the ratio of the time during which a given cluster exists to the entire time of the simulation.

The kinetics of aggregation is followed by cluster analysis, carried out with the method of single linkage, which uses similarity of atomic coordinates to assign molecules to an aggregate. The cutoff, which has the meaning of the largest interatomic distance between the closest atoms of neighboring molecules in a cluster, is taken as the end of the first peak of the minimum distances distributions (see below). This analysis yielded a value 0.28 nm, which is employed as a limiting distance when determining cluster sizes. Notably, it coincides with the full width at half-maximum of the radial distribution function (RDF) between the centers of mass of neighboring BS molecules within stable dimers, which agrees with the findings from a very detailed general analysis of RDFs.[40]

## RESULTS AND DISCUSSION

The aggregation behavior of the studied molecules is compared by estimating the times necessary for the formation of the largest aggregates within the model, their persistence in time, and the nature of the forces acting between the molecules. Representative aggregates of each BS are analyzed in more detail to calculate their size, shape, and type of stabilizing intermolecular interactions.

**Cluster Analysis: Aggregation Numbers and Kinetics of Formation.** The evolution of the size of the largest cluster for all BS is shown in Figure 2. It reveals a systematic increase of the aggregates' size with time. Only for CH and TDCH a larger cluster dissociates temporarily to a smaller one (a pentamer to a tetramer) but is restored in ca. 20 ns. For the time of the simulations the nonconjugated salts and the tauro conjugates form stable pentamers while the glyco derivatives yield a hexamer (GCH) and an octamer (GDCH). The time required to form a stable pentamer is the shortest for TDCH (6 ns) and the longest for TCH (109 ns). CH and DCH aggregate within intermediate times: 48 and 87 ns, respectively. GCH assembles into a stable hexamer for 31 ns, and this is the only system for which no long-living pentamer is registered. The stable octamer of GDCH is formed for 77 ns. Both types of conjugated molecules (tauro and glyco) aggregate faster than the nonconjugated ones. It should be noted that all kinetics results should be interpreted in a qualitative manner as relative data for the different salts. The numbers provided above can be absolute quantitative indicators only if they stem from a large number of NVT MD simulations for each system, which is hardly plausible at the current state of computational power. Nevertheless, they reflect appropriately the aggregation specificity of the various bile salts.

Increase of the aggregates' size takes place by gradual addition of monomers to the largest micelle already formed and not by merging of smaller clusters. For a very short time (during the relaxation or shortly after that) the initially randomly placed BS molecules self-assemble into dimers, which are very dynamic and frequently exchange molecules with the bulk. The dimer of TDCH is the only exception: once formed, it persists for about 6 ns when three more molecules associate to it to give a pentamer.

To reveal the reason for this pronounced stability of the TDCH dimer, the properties of dimers of the six BS, which were stable for 996 ps in the initial phase of the simulations (the first 4 ns), were analyzed. The number of contacts and the minimum interatomic distance (within a cutoff of 0.30 nm) between atoms of the two molecules in each dimer for the whole period were determined first. The results are summarized in Figure 3. It is evident that the atoms in the TDCH dimer are


DOI: 10.1021/acs.jpcb.5b07063
J. Phys. Chem. B 2015, 119, 15631−15643

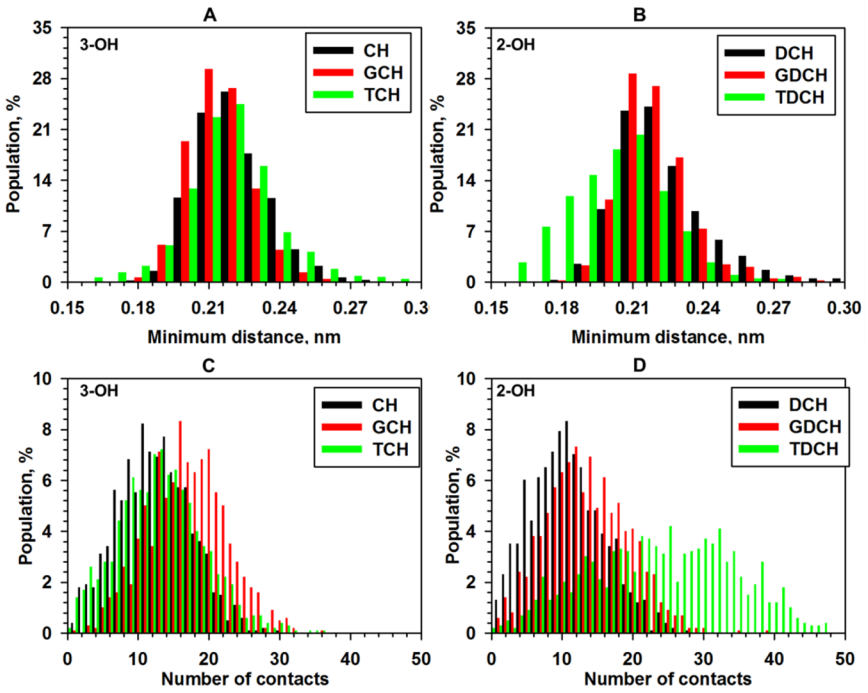


**Figure 3.** (A, B) Minimum distances per picosecond and (C, D) number of atomic contacts per picosecond between the molecules in the dimers formed at the beginning of the simulations by the six bile salts.

at much shorter distances than those in the other dimers, which naturally results in a much higher number of contacts. Moreover, the distribution of the number of contacts there is much broader than in the other systems indicating that a larger number of favorable orientations of the two molecules exist in the TDCH dimer. The average number of contacts in this dimer is ≈24, for GCH it is ≈16, and for the rest of the dimers it is between 11 and 13. The difference for the dimers of TCH and TDCH is twice (12 vs 24 contacts), even though the two molecules differ in one hydroxyl group only.

Next, the most probable relative orientation of the two molecules within the dimers was estimated. A vector shown in Figure 4A was defined for each molecule. It was chosen because it connects the two outermost atoms of the steroid fragment, which is an identical rigid part of all molecules. The variation of the angle between the vectors of the two molecules for the period of stability of the dimers of TCH and TDCH is presented in Figure 4B.

This analysis reveals that up to 200 ps the most probable angle between the two TCH or TDCH molecules is about 155°. After that a conformational transition takes place leading to a decrease of the angle to ca. 70° for TCH and to ca. 10° for TDCH. After 400 ps the angle in the TCH dimer is restored to about 155° and fluctuates around this value until the separation of the two molecules. On the contrary, the angle in the TDCH dimer relaxes to about 35° and varies around this magnitude (Figure 4B). To provide an explanation for this contrasting behavior, the intermolecular hydrogen bonds in the dimers of TCH and TDCH were analyzed. It was found that there is practically no H-bonding in the former whereas two hydrogen bonds (denoted in Figure S3 of the Supporting Information) exist in the dimer of TDCH for 65% of the trajectory (996 ps) of this dimer. Therefore, the dimer of TDCH owes its stability to these two intermolecular hydrogen bonds. The more resistant dimer of TDCH leads to faster aggregation up to a stable pentamer within 6 ns.

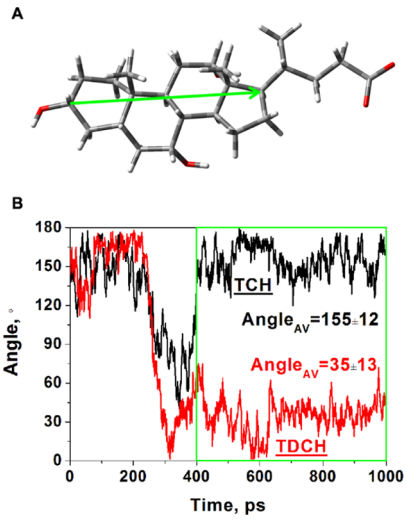


**Figure 4.** (A) Illustration of the vector used to assess the intermolecular orientation of BS in the aggregates. (B) Evolution of the angle formed between the vectors of the two molecules in a dimer of TCH (black) and TDCH (red) for a period of 996 ps.

In contrast, in the dimer of TCH the molecules interact only through their hydrophobic steroid rings, which renders their separation easier. Breaking this dimer is facilitated further by the pronounced hydrophilicity of TCH. Due to this, a stable pentamer of the taurocholate is formed only after 100 ns, and the molecular behavior therein is different from that in the pentamers of the other BS. The main difference stems again from the number of intermolecular contacts in the aggregates, which is much smaller for TCH, as discussed below (Table 3).

Trimers are not abundant in any of the studied systems, which is seen from the size distribution of the aggregates shown in Figure 5. Tetramers are also short-lived (except for TCH). This is due to the fact that 3 or 4 molecules are not sufficient



DOI: 10.1021/acs.jpcb.5b07063
J. Phys. Chem. B 2015, 119, 15631−15643

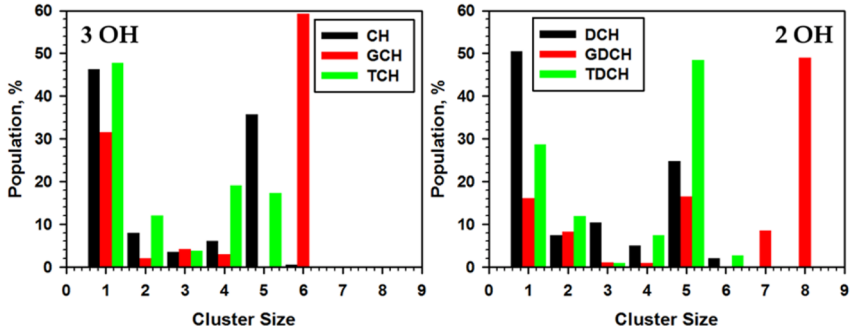


**Figure 5.** Histograms of cluster size normalized for 150 ns of simulation showing the relative population of the BS molecules in aggregates with different size. The plot on the left is a comparison of the trihydroxy salts, and that on the right is of the respective dihydroxy derivatives.

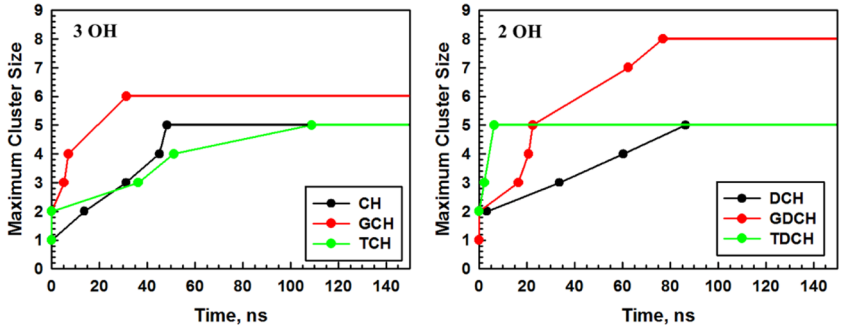


**Figure 6.** Comparison of the kinetics of micelles formation of the studied bile salts as a function of the number of hydroxyl groups (left vs right) and of the type of hydrophilic head (colors).

for efficient packing of all hydrophobic parts away from the water molecules. The tetramer of TCH is relatively stable because this molecule has the largest hydrophilic surface area, and four molecules are sufficient to shield the hydrophobic fragments. They survive for ca. 60 ns, and then a pentamer forms, which remains stable until the end of the simulation. This result is in very good agreement with literature data[3] providing an aggregation number of 4.5 for TCH.

In almost all systems studied the largest aggregates formed are also the longest-living. The exceptions are the nonconjugated molecules, for which monomers are the most populated due to their generally slower self-assembly. Nevertheless, intensive dynamics and stepwise increase of the size of the aggregates is witnessed for all BS. Since the aggregation could in principle depend on the choice of the thermodynamic ensemble, we have run also a 100 ns NPT simulation (at pressure of 1 bar and the same temperature as in the NVT calculation) for one of the studied systems, the solution of TDCH. Some key results are summarized in Figures S4 and S5 of the Supporting Information. Both in NVT and in NPT the molecules of TDCH aggregate stepwise and reach a stable pentamer and hexamer, respectively. As could be expected, the initial times of formation of the pentamer are different in the two trajectories, but nevertheless, it assembles quite fast (at ca. 23 ns) in the NPT simulation as well. In both simulations the largest population belongs to the largest cluster formed and the smallest one to a trimer (Figure S4B). The overall distributions are alike, too. Analysis performed for the pentamers from the two simulations shows very similar hydrogen bonding and dispersion interaction patterns (Figure S5). So, it is assumed that the influence of the ensemble is small.

Unlike the nonconjugated salts and the tauro conjugates, which form stable pentamers, the glyco derivatives yield aggregates of larger size: a hexamer for GCH and an octamer for GDCH. GCH is the only salt without a stable pentamer. In a very short time a hexamer is formed, which perseveres until the end of the simulation. This indicates that more than five GCH molecules need to pack in order to provide an energetically favorable configuration. The necessity of a larger number of molecules probably comes from the larger size of this ion compared to the nonconjugated one and from the smaller hydrophilic head compared to the tauro derivatives. The participation of the hydrophilic head of GCH into the aggregation process is addressed in more detail below. In the GDCH models the molecules gradually group to grow to a trimer (Figure 2), a tetramer, a pentamer, and a heptamer within 77 ns, after which a stable octamer forms persisting for 73 ns until the end of the simulation. It cannot be claimed that 8 is the aggregation number of GDCH because of the limitation of the model, but this is the only system where the maximum possible cluster size is reached, which is in an agreement with the experimental data by Small and co-workers,[3] who obtained the largest $N_{agg}$ for this system as well (Table 1).

The tendency for the nonconjugated salts resembles that of the glyco conjugates. Both CH and DCH form stable pentamers. DCH indicates a possibility for aggregation into a larger cluster, a hexamer, which exists during the last 2 ns of the simulation.

The aggregation numbers observed within the current models are 5 for CH and TCH and 6 for GCH. DCH and TDCH also form stable pentamers, and GDCH, an octamer. The results obtained for the trihydroxy derivatives agree very well with experimentally determined $N_{agg}$ known in the literature (Table 1). The aggregation numbers of the dihydroxy representatives found in the present work, however, are much smaller than those derived from experimental data. This may be


DOI: 10.1021/acs.jpcb.5b07063
J. Phys. Chem. B 2015, 119, 15631−15643

interpreted as more pronounced affinity of the dihydroxy BS toward formation of secondary micelles. It should be noted that aggregation numbers cannot be determined unambiguously within this study since the simulations are stopped at 150 ns. Another limiting factor is the size of the models, each of which contains 8 BS molecules only. Investigation of the larger possible aggregation numbers is planned in the next stage of the study by coarse-grained MD. Here, mostly relative numbers are discussed, and when absolute values are given, they should be regarded within the limitations of the model.

The influence of the number of hydroxyl groups on the size of the aggregates and on the rate of aggregation is illustrated in Figure 6 where the symbols denote the moment of formation of the clusters with different size. Although the dihydroxy salts are characterized with higher $N_{agg}$, their aggregation appears slower than that of the trihydroxy molecules in the nonconjugated and in the glyco derivatives. The tauro conjugates deviate from this trend since TCH self-assembles comparatively slowly and TDCH has the fastest aggregation among all studied systems. This mismatch of the kinetic trends between the di- and trihydroxy salts might stem from the initial random placement of the molecules in the periodic box. In order to eliminate the influence of the starting structure during the initial stage of the aggregation, 20 ns simulations were carried out for all bile salts using identical starting configurations. The results are summarized in Figure S6 of the Supporting Information. The profiles do not differ much from the first 20 ns in Figure 2, but a more uniform trend is witnessed. The micelles of TDCH and GDCH grow faster than those of TCH and GCH. This indicates speedier self-assembly of the dihydroxy conjugates. Only dimers of CH and DCH exist during these simulations, which reflects their slower aggregation kinetics. Inspection of the dimers confirmed the conclusion made above, that the dimers of TCH are very mobile while in TDCH a fixed orientation prevails. Hence, it can be assumed that this alignment is preferential for faster aggregation.

However, dominant intermolecular alignment is not retained in the larger stable clusters. There is no fixed relative orientation of the molecules within the micelles. Expectedly, the most frequent alignment of neighboring molecules is facing the hydrophobic parts of their steroid rings, which corresponds to literature data from other theoretical studies.[16−18] This is seen most clearly in the dimers (Figure S3, right). In most of the dimers the methyl groups of the two molecules are somewhat displaced, and the hydrophilic heads are solvated by water molecules. This preferred orientation can be explained by the fact that the heads are negatively charged, and hence, their face-to-face orientation is electrostatically unfavorable. In the larger clusters of all BS the hydrophilic heads remain located primarily at the periphery of the micelle, pointing toward water, which corroborates their enhanced hydrophilic nature. This casts some doubt on the possibility for formation of intermolecular hydrogen bonds within the clusters, which some literature sources[3,15,41] delineate as the main reason for stabilization of BS micelles. Detailed analysis of H-bonding is presented in the next section.

It should be noted, however, that no orientational ordering of the molecules takes place within the aggregates (Figure 7). Neighbors can close different angles with each other. This is confirmed by analysis of the angle between the vectors defined longitudinally for each molecule within a given aggregate (Figure 4). The evolution of this angle is monitored for all pairs of molecules, and it spans the entire range from 0° to 180° (a representative example is shown in Figure S7 of the Supporting Information). This means that there is no preferred intermolecular orientation in any of the micelles and implies that the BS micelles could easily rearrange their structure in order to host suitable hydrophobic hosts such as cholesterol.

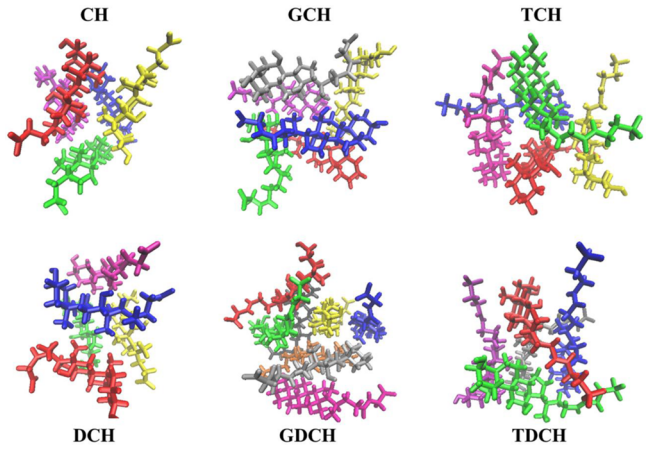


**Figure 7.** Illustration of the most populated clusters of all BS: pentamers of CH, DCH, TCH, and TDCH; hexamer of GCH; and octamer of GDCH.

In order to characterize the type of interactions between the BS molecules within the aggregates, the most stable clusters of the six salts were compared for identical period of time, 30 ns, selected as the optimum time during which a stable micelle exists in all systems. For correct comparison, all quantities (number and length of hydrogen bonds, number and length of intermolecular distances describing hydrophobic interactions) are calculated for the entire cluster and then normalized for one molecule.

**Hydrogen Bonds.** Intermolecular hydrogen bonds between BS in their aggregates are discussed extensively in the literature[3,15,41] as one of the main driving forces stabilizing the micelles. The presence of several hydroxyl groups (2 or 3) and a carboxyl, glycyl, or tauryl residue in these molecules enables formation of hydrogen bonds, which may stabilize the clusters.

Therefore, the hydrogen bonds within each representative aggregate of the six studied BS were evaluated. The H-bonds between BS and water molecules were calculated, too. A proton/H-acceptor cutoff = 0.35 nm and maximum limiting angle proton/H-donor/H-acceptor of 30° were used. Distributions of the number of hydrogen bonds between BS molecules within the clusters are given in Figure 8, and the average number of H-bonds of BS with water is summarized in Table 2.

It is seen that the most probable number of H-bonds between BS molecules is small: formation of 1 or 2 hydrogen bonds is the most likely (2 or 3 for GDCH). However, the maximum probability per molecule is around 7% for the tauro derivatives and much less for the other molecules in spite of the fact that each of them contains at least 4 electronegative atoms, which may bind some of the available protons (minimum 2). This negligible affinity toward hydrogen bonding inside the clusters can be rationalized in terms of the micelles' structure: the molecules turn preferably their hydrophilic parts toward water aiming to shield as much as possible the hydrophobic fractions from it (Figure 9).

Hydrogen bonds between the molecules of cholate and deoxycholate will not be discussed because their average


DOI: 10.1021/acs.jpcb.5b07063
J. Phys. Chem. B 2015, 119, 15631−15643

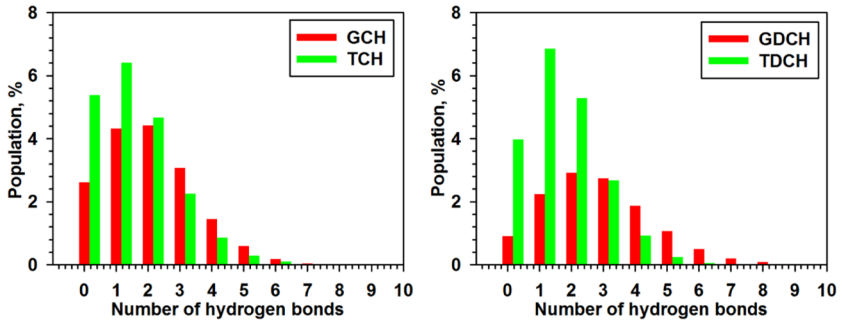


**Figure 8.** Probability of formation of different numbers of hydrogen bonds within the aggregates of GCH (hexamer), GDCH (octamer), TCH (pentamer), and TDCH (pentamer) for a period of 30 ns; the population data are normalized per molecule and per picosecond. No values are shown for the nonconjugated molecules because they practically do not form such hydrogen bonds (Table 2).

**Table 2. Average Number (with Standard Deviation) and Most Probable Length of BS−BS and BS−Water Hydrogen Bonds (HBs) Formed by One BS Molecule in the Aggregates**

| molecule | $N_{agg}^{calc}$ | no. of BS−BS HBs | length, nm | no. BS−water HBs | length, nm |
|---|---|---|---|---|---|
| CH | 5 | 0.08 ± 0.13 | 0.17 | 15 ± 1 | 0.18 |
| DCH | 5 | 0.06 ± 0.11 | 0.18 | 13 ± 1 | 0.18 |
| GCH | 6 | 0.33 ± 0.23 | 0.17 | 16 ± 1 | 0.18 |
| GDCH | 8 | 0.28 ± 0.19 | 0.18 | 14 ± 1 | 0.18 |
| TCH | 5 | 0.28 ± 0.26 | 0.19 | 17 ± 1 | 0.19 |
| TDCH | 5 | 0.33 ± 0.24 | 0.19 | 14 ± 1 | 0.19 |

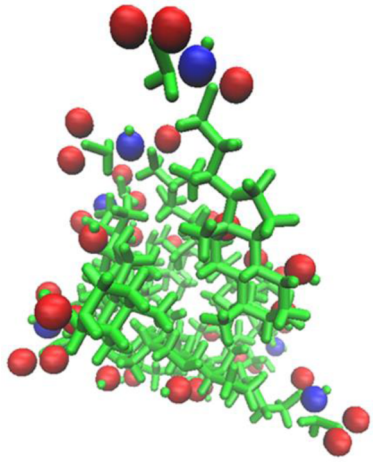

**Figure 9.** Illustration of the micellar structure on the example of a GCH hexamer. The hydrocarbon skeleton is colored green, the oxygen atoms red, and the nitrogen atoms blue.

number for the entire pentamers is less than 0.1 (Table 2), and therefore, we assume that H-bonding is negligible in these micelles. This conclusion contradicts the statement by Partay et al.[15] that hydrogen bonding is significant in the primary micelles of cholate.

There might be several reasons for this discrepancy. First, the different force field/water model combinations (united-atom with SPC/E in the study of Partay et al. vs all-atom with TIP3P in the current work) are likely to result in different balance of the nonbonded interactions. This is confirmed by a recent detailed comparative study of the two types of force fields for the description of a surfactant micelle.[42] There, AMBER99SB and the newer versions of GROMOS are shown to reflect adequately the micellar properties. Second, Partay and coauthors[15] use distance criteria for hydrogen bonding. This assumption takes into account only implicitly the angular component of H-bonds, which exists in the official definition.[43] Hence, the H-bonding criterion in the current study is somewhat more stringent. It should also be mentioned that their simulations are carried out at room temperature where the dynamics of molecules is slower and more H-bonds could be stabilized. Last but not least, the simulation times of Partay et al. are much shorter, and given the slower aggregation with GROMOS,[42] and the fact that H-bonds were observed predominantly in cholate dimers, this may well be a reflection of the earlier stages of CH self-assembly. To test this, the intermolecular hydrogen bonds were calculated within a CH dimer existing in the period 13.5−29.0 ns in our trajectory. H-bonds were seen to form and break occasionally, with their average number being 0.03 ± 0.22, which is in the range reported by Partay et al. All this indicates that the negligible hydrogen bonding in the most stable micelles of CH and DCH registered in the present work is realistic for the conditions studied herein. Apart from H-bonding, the two studies agree quite well in terms of aggregates' size and relative behavior of CH and DCH.

The distribution of the number of H-bonds in BS clusters (Figure 8) signposts the assumption that these bonds involve electronegative atoms from the hydrophilic heads. After additional analysis of the H-bond donors and acceptors, it is found that almost all possible combinations appear. It is noteworthy that the peptide amino group often participates, binding either with atoms from the hydrophilic head or from the hydroxyl groups attached to the steroid part of a neighboring molecule. Its absence in CH and DCH may be the reason for the lack of hydrogen bonding there. This variety of H-bonds in the micelles of the conjugates is an additional corroboration of the idea of intensive dynamics of the clustered molecules allowing a multitude of feasible conformations. On the other hand, the broader distributions of the glyco conjugates (2 or 3 most probable bonds and up to 8 H-bonds in total in some clusters) may explain their faster aggregation and higher aggregation numbers.

To evaluate the influence of hydrogen bonding as a stabilizing factor for the aggregates, the total lifetime of the various hydrogen bonds formed within 30 ns of the trajectory of a given aggregate is calculated for the two nonconjugated and for the two glyco derivatives. The total lifetime is the overall time for which a certain hydrogen bond exists in the analyzed part of the MD trajectory. The graphs (Figure 10) illustrate clearly the difference between CH/DCH, on one hand, and GCH/GDCH, on the other hand. In the micelles of


DOI: 10.1021/acs.jpcb.5b07063
J. Phys. Chem. B 2015, 119, 15631−15643

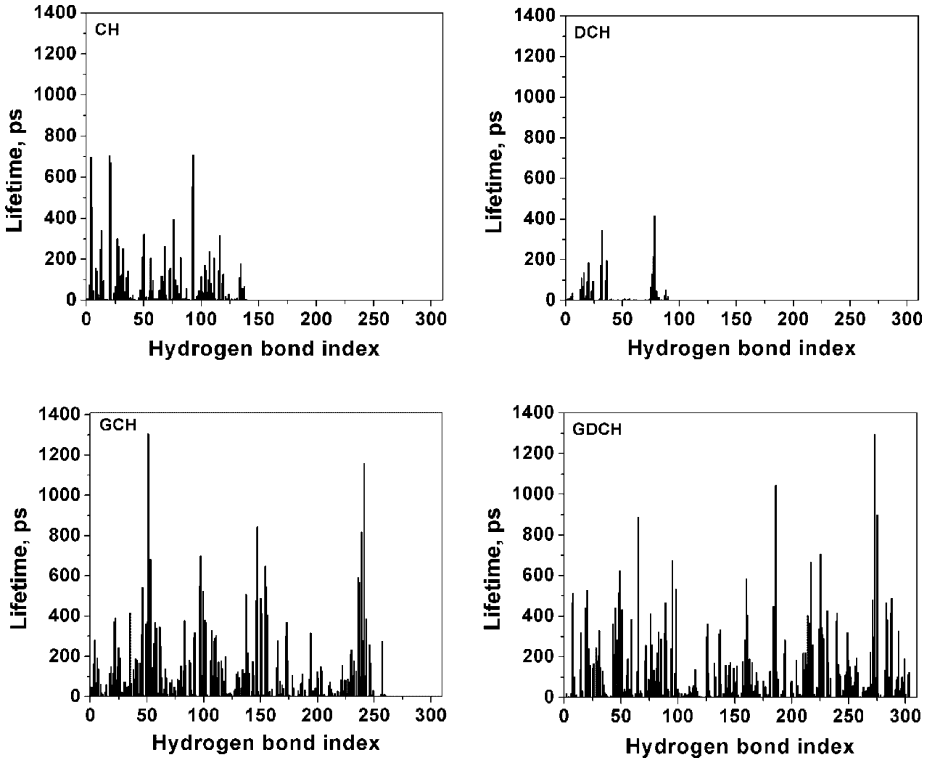


**Figure 10.** Total lifetimes of the various H-bonds existing during 30 ns of the trajectory of the representative clusters of CH, DCH, GCH, and GDCH; every hydrogen bond index corresponds to a different triplet donor−H−acceptor.

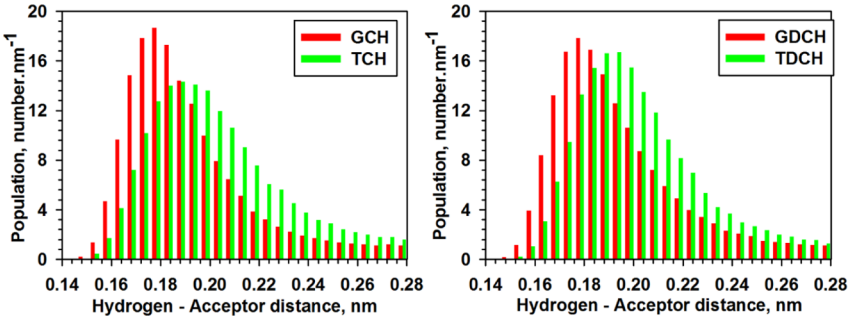


**Figure 11.** Distributions of the lengths of intracluster hydrogen bonds for the 30 ns taken from the trajectory of the representative aggregates: pentamers of TCH and TDCH, hexamer of GCH, and octamer of GDCH. The data are normalized per BS molecule.

the nonconjugated salts there are 138 different H-bonds in the pentamer of CH and 90 bonds in that of DCH, whereas these numbers are 261 for the hexamer of GCH and 302 for the octamer of GDCH. These much more abundant hydrogen bonds in the micelles of GCH and GDCH cannot be due only to the slightly larger number of molecules therein. On average, the lifetimes are also longer in the aggregates of the glyco conjugates than in those of CH and DCH.

This qualitative difference between the two types of molecules comes from the presence of the additional donor in the glyco derivatives: the peptide group, which takes part in many hydrogen bonds (47% for GCH), mostly with protons from the steroid hydroxyl groups. Having in mind that hydrogen bonding is longer-range than van der Waals interactions, this preference for hydrogen bonding can explain the faster aggregation of the glyco derivatives compared to that of nonconjugated molecules where H-bonds are virtually missing.

The distributions of H-bond lengths are given in Figure 11. It is interesting that the most populated length of hydrogen bonds between all types of BS molecules varies in a narrow range: 0.17−0.19 nm. The shorter bonds (around 0.17 nm) are characteristic for the glyco conjugates, and the longer ones (around 0.19 nm) are characteristic for the tauro derivatives, which is another dissimilarity resulting from the two different heads. It should be due to the bulkier sulfate group of taurine. The fact that the H-bonds of the glyco conjugates are stronger contributes definitely to their larger aggregation numbers (6 and 8) and faster self-assembly.

Nevertheless, overall the intra-aggregate hydrogen bonds are not abundant and are broken ferquently.

The H-bonds between BS and water, on the other hand, are much bigger in number, 14−17 per BS molecule (Table 2), and it fluctuates slightly around a constant average value. This means that the salts always form strong hydrogen bonds with the surrounding water molecules. The most populated H-bond lengths are the same as those within the aggregates, which



DOI: 10.1021/acs.jpcb.5b07063
J. Phys. Chem. B 2015, 119, 15631−15643

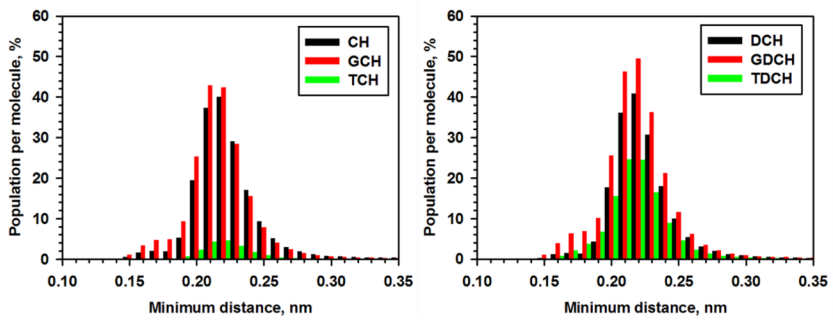


**Figure 12.** Distributions of the minimum distances between all pairs of molecules in the pentamers of CH, DCH, TCH, and TDCH; the hexamer of GCH; and the octamer of GDCH. All data are normalized per one molecule and per one picosecond.

indicates that these distances are typical for bile salts. Hence, such a length can be expected also for H-bonds in the secondary micelles, which are widely discussed in the literature.[3,41]

The formation of a few intermolecular hydrogen bonds between BS and the small aggregation numbers registered in the present study indicate that the observed aggregates correspond to the so-called *primary micelles*. This is due to the very low concentration, on one hand, and to the limited simulation time, on the other. However, it does not impede the extraction of valuable information from the atomistic study.

Small and co-workers[3] have tested experimentally the presence of hydrogen bonds in BS micelles by adding 4 and 6 M urea, a known H-bond breaker, to micellar solutions of various bile salts with different aggregation numbers. They have established that the typically higher aggregation numbers of dihydroxy salts decreased substantially (from 63 to 6 for GDCH). $N_{agg}$ of the trihydroxy derivatives also decreased (down to 2). These results demonstrate that hydrogen bonds may be important for stabilization of the aggregates. However, it should be stressed that urea is known to break the hydrophobic interactions as well, because the latter also have their origin in the hydrogen bonds between water molecules.[44]

**Intermolecular Hydrophobic Interactions within the Micelles.** The predominant hypothesis in the literature with respect to stabilizing forces in bile salts aggregates is that they are hydrophobic.[4] To check this, quantitative analysis of these interactions was made for the most stable aggregates of the six BS. The minimum interatomic distances (up to a cutoff of 0.60 nm) between all pairs of molecules constituting a cluster were determined, which permitted quantitative assessment of the hydrophobic intermolecular coupling. The results are given as histograms in Figure 12.

In each analyzed aggregate the most populated minimum distance is 0.22 or 0.23 nm, with the more probable values spanning the range from 0.19 to 0.26 nm. These distances are of the order of the sum (0.24 nm) of the van der Waals radii of two hydrogen atoms. This shows that the BS molecules in the micelles are tightly packed and form a hydrophobic medium where no water molecules penetrate. It is important to note that the population of the minimum distances, which reflects the number of intermolecular contacts (Table 3), is much lower for the tauro conjugates than for the unconjugated salts. The difference is spectacular for TCH. The analysis of intracluster H-bonds for this molecule also showed that they are the fewest at the expense of the more abundant H-bonds with the water molecules. All these factors outline the micelles of TCH as the most labile among the studied systems. TDCH is in an intermediate position because its aggregates are moderately stabilized by hydrophobic interactions and by intracluster H-bonds.

**Table 3. Number of Contacts (with Standard Deviation) and Most Probable Intermolecular Separation between the Aggregated BS Molecules, Averaged over the 30 ns Taken from the Trajectory of the Representative Clusters**

| molecule | $N_{agg}^{calc}$ | no. of contacts per molecule | most probable separation, Å |
|---|---|---|---|
| CH | 5 | 753 ± 64 | 2.2 |
| DCH | 5 | 729 ± 61 | 2.2 |
| GCH | 6 | 1584 ± 209 | 2.1 |
| GDCH | 8 | 1035 ± 55 | 2.2 |
| TCH | 5 | 264 ± 82 | 2.2 |
| TDCH | 5 | 1137 ± 220 | 2.1 |

From a comparison of the distributions of the number of hydrogen bonds between BS molecules, which is from 0 to 1 per molecule (Table 2), and the number of contacts between the hydrophobic residues of the aggregated molecules, which are in the range 300−1500 per molecule (Table 3), it can be concluded that the stabilizing forces acting between the molecules in the BS micelles are the hydrophobic ones. This conclusion is in accordance with literature data and hypotheses that hydrophobic interactions dominate the self-assembly process of bile salts in diluted aqueous solutions.[4,18]

For the initial stage of the aggregation process, which is tackled within this study, namely, the formation of primary micelles, the intermolecular hydrogen bonds can be regarded only as a kinetic driving force for faster aggregation of the glyco and tauro conjugated derivatives.

Bearing in mind the lack of preferred intermolecular orientation in the micelles, the fast molecular dynamics therein, the hydrophobic core, and the fact that the molecules are coupled mainly by the soft dispersive interactions, the pronounced capacity of these aggregates for solubilization of liophilic substances could be explained by their readiness to readjust given an appropriate hydrophobic guest molecule.

**Size and Shape of the Aggregates.** Among the most often discussed characteristics of BS micelles for many years[4,5,16−18] are their size and shape. As described in the Introduction, a number of hypotheses have been formulated about the most probable shape and the likely size, based on different experimental and theoretical data. However, there is no clear picture on the subject to date. It is known that BS aggregates are fairly different from the micelles of conventional surfactants and that their shape depends on the concentration


DOI: 10.1021/acs.jpcb.5b07063
J. Phys. Chem. B 2015, 119, 15631−15643

of the bile salts and on the experimental conditions, such as temperature, pH, or ionic strength.

To define the shape of the micelles, the ratios between the moments of inertia were used in the present study, and the radius of gyration ($R_g$) served as a measure of the size. The evolution of $R_g$ along the trajectory of the representative aggregates is shown in Figure 13.

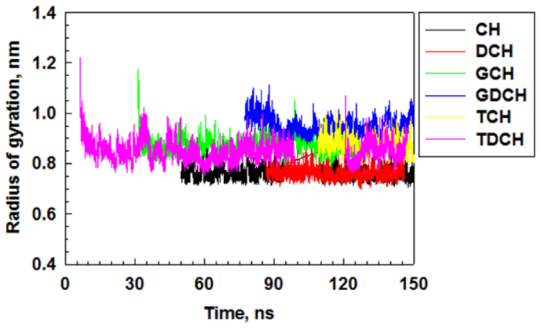


**Figure 13.** Evolution of the radius of gyration of the most stable aggregates of the six bile salts along their trajectory: CH, DCH, TCH, TDCH pentamer; GCH, hexamer; GDCH, octamer.

It is evident that after a short relaxation of the clusters for ca. 2 ns, which serve for intracluster reorganization, the radius of gyration of all micelles starts fluctuating around a constant average value. The fluctuations are somewhat more expressed for the conjugated derivatives than for CH and DCH, which is due to the longer hydrophilic heads located in water, but in general, all values span similar ranges. Long-time fluctuations of $R_g$ are visible, in line with the dynamic structure of the clusters.

The average sizes of the BS micelles (Table 4) are very small: the radii are close to 1 nm. The pentamers of CH and DCH have identical size. $R_g$ values of the pentamers of TCH and TDCH are also similar and larger than those of the nonconjugated clusters. The hexamer of GCH is as large as the pentamer of TCH, which is most likely due to the smaller size of the glycine residue. Expectedly, the octamer of GDCH is the largest (Table 4). In spite of the small differences for the various BS, the radii of their micelles vary in a very narrow range, 0.76−0.95 nm, which stems from the similar dimensions of the constituting molecules. The experimentally determined radius in the work of Woodford et al.[7] of 1 nm for TCH micelles with aggregation number 5 falls very close to this range. Similar small sizes have been obtained also for aggregates of TDCH (1−1.2 nm) with $N_{agg}$ = 22 (secondary micelles) by ultracentrifugation and gel filtration,[5,6] which indicates that our model systems are a good representation of the real ones.

To verify further the obtained numerical results, we conducted an experiment to measure the size of TDCH aggregates with dynamic laser light scattering (DLS). Samples of TDCH with concentration 100, 50, and 25 mM in 120 mM NaCl were measured, since concentration of 10 mM is below the apparatus sensitivity. Even the solutions with 10 times higher concentration gave rise to very weak signals, which shows that the sizes are below 2 nm (the sensitivity threshold of the machine). This result confirms the outcome from the simulations.

The moments-of-inertia ratios are interpreted in general as follows: $I_x/I_y \approx 1$ and $I_y/I_z \approx 1$ correspond to spherical shape; when $I_x/I_y \approx 1$ and $I_y/I_z \ll 1$, the shape is disc-like. In the cases $I_x/I_y \ll 1$ and $I_y/I_z \approx 1$, the micelles are rod-like. In the studied systems the former ratio is close to 0.7, and the latter is about 0.9. These ratios indicate that BS micelles can be modeled as ellipsoids or deformed spheres, which is confirmed also by visual inspection of the MD trajectories. This is in close agreement with previous findings about the shape of BS micelles.[17,18]

The registered specificity of all BS micelles, very small size and irregular shape (deformed sphere or ellipsoid), may be explained with the ability of the BS molecules to pack while being oriented in various ways with respect to each other. This is enabled by their special "two-faced" chemical structure. As already mentioned, this flexibility of orientation probably facilitates the solubilization of hydrophobic molecules *in vivo*. The present detailed analysis at the atomistic level confirms the hypothesis of Verde and Frenkel[18] who state the same on the basis of coarse-grained MD simulations of BS aggregation.

## CONCLUSIONS

Fully atomistic molecular dynamics simulations of the aggregation process of six bile salts, encountered in human organisms, are carried out under conditions mimicking those in the human gastrointestinal tract. The modeled molecules differ in the number of hydroxyl groups (two or three) in the steroid skeleton and in the type of their hydrophilic head. All simulations are in aqueous solution, at 37 °C, in the presence of 120 mM NaCl with concentration of the bile salts 10 mM which is the physiological range found in humans. Small primary micelles are formed in all systems on the time scale of 6−110 ns. These micelles have radii about 1 nm and aggregation numbers between 5 for nonconjugated and tauro conjugated cholate and deoxycholate, and 6−8 for glyco conjugates. The bile salts aggregates are stabilized by hydrophobic interactions between the steroid rings, whereas intermolecular hydrogen bonds are few and do not affect substantially the stability of the primary micelles. The intermolecular hydrogen bonds serve, however, to speed up the aggregation of conjugated bile salts. The reason for the faster self-assembly of taurodeoxycholate, glycodeoxycholate, and glycocholate is the formation of intracluster hydrogen

**Table 4. Average Radii of Gyration ($R_g$'s) and Ratios of Moments of Inertia ($I_j$) along the Three Spatial Directions for All Representative BS Aggregates**

| molecule | $N_{agg}^{calc}$ | $R_g$, nm | $I_x/I_y$ | $I_y/I_z$ | $I_x/I_z$ |
|---|---|---|---|---|---|
| CH | 5 | 0.76 ± 0.03 | 0.72 ± 0.13 | 0.87 ± 0.06 | 0.62 ± 0.10 |
| DCH | 5 | 0.76 ± 0.02 | 0.72 ± 0.12 | 0.88 ± 0.06 | 0.63 ± 0.09 |
| GCH | 6 | 0.87 ± 0.03 | 0.67 ± 0.13 | 0.88 ± 0.06 | 0.58 ± 0.10 |
| GDCH | 8 | 0.95 ± 0.03 | 0.77 ± 0.12 | 0.87 ± 0.06 | 0.60 ± 0.10 |
| TCH | 5 | 0.87 ± 0.03 | 0.70 ± 0.12 | 0.84 ± 0.06 | 0.59 ± 0.09 |
| TDCH | 5 | 0.85 ± 0.04 | 0.71 ± 0.12 | 0.86 ± 0.07 | 0.61 ± 0.09 |



DOI: 10.1021/acs.jpcb.5b07063
J. Phys. Chem. B 2015, 119, 15631−15643

bonds, involving the nitrogen atom from the hydrophilic head and a proton from another molecule.

The molecules within the aggregates are very dynamic; the micelles core is entirely hydrophobic and does not tolerate inclusion of water molecules. These features of aggregates may be considered important for the profound capacity of bile salts micelles to solubilize hydrophobic molecules, such as cholesterol, fatty acids, and alkylmonoglycerides *in vivo*.

All aggregates have irregular shapes, which can be approximated as ellipsoids or deformed spheres. Glyco conjugates yield the largest micelles (a hexamer and an octamer) while pentamers are characteristic for the non-conjugated salts and for the tauro conjugates. The obtained theoretical estimates are in very good agreement with experimental data and provide new important insights into the bile salts aggregation mechanism and its specifics.

## ■ ASSOCIATED CONTENT

### Supporting Information

The Supporting Information is available free of charge on the ACS Publications website at DOI: 10.1021/acs.jpcb.5b07063.

Additional figures, including illustrations of molecular models, structures, and kinetic data, and additional tables, with force field parameters, RESP atomic charges, atomic connectivity information, and atom types (PDF)

## ■ AUTHOR INFORMATION


### Corresponding Author

*E-mail: aivanova@chem.uni-sofia.bg. Phone: ++35928161520. Fax: ++35929625438.


### Notes

The authors declare no competing financial interest.

## ■ REFERENCES


(1) Gouin, S.; Zhu, X. X. Fluorescence and NMR Studies of the Effect of a Bile Acid Dimer on the Micellization of Bile Salts. *Langmuir* **1998**, *14*, 4025−4029.

(2) Poša, M.; Sebenji, A. Determination of Number-average Aggregation Numbers of Bile Salts Micelles with a Special Emphasis on their Oxo Derivatives-The Effect of the Steroid Skeleton. *Biochim. Biophys. Acta, Gen. Subj.* **2014**, *1840*, 1072−1082.

(3) Small, D. M. Size and Structure of Bile Salt Micelles. *Adv. Chem. Ser.* **1968**, *84*, 31−52.

(4) Carey, M. C.; Small, D. M. Micelle Formation by Bile Salts. Physical-chemical and Thermodynamic Considerations. *Arch. Intern. Med.* **1972**, *130*, 506−527.

(5) Laurent, T. C.; Persson, H. A. Study of Micelles of Sodium Taurodeoxycholate in the Ultracentrifuge. *Biochim. Biophys. Acta, Lipids Lipid Metab.* **1965**, *106*, 616−624.

(6) Borgstrom, B. The Dimensions of the Bile Salt Micelle. Measurements by Gel Filtration. *Biochim. Biophys. Acta, Lipids Lipid Metab.* **1965**, *106*, 171−183.

(7) Woodford, F. P. Enlargement of Taurocholate Micelles by Added Cholesterol and Monoolein: Self-diffusion Measurement. *J. Lipid Res.* **1969**, *10*, 539−545.

(8) Matsuoka, K.; Suzuki, M.; Honda, C.; Endo, K.; Moroi, Y. Micellization of Conjugated Chenodeoxy- and Ursodeoxycholates and Solubilization of Cholesterol into their Micelles: Comparison with Other Four Conjugated Bile Salts Species. *Chem. Phys. Lipids* **2006**, *139*, 1−10.

(9) Funasaki, N.; Nomura, M.; Ishikawa, S.; Neya, S. Hydrophobic Self-association of Sodium Taurochenodeoxycholate and Tauroursodeoxycholate. *J. Phys. Chem. B* **2000**, *104*, 7745−7751.

(10) Ninomiya, R.; Matsuoka, K.; Moroi, Y. Micelle Formation of Sodium Chenodeoxycholate and Solubilization into the Micelles: Comparison with Other Unconjugated Bile Salts. *Biochim. Biophys. Acta, Mol. Cell Biol. Lipids* **2003**, *1634*, 116−125.

(11) Sugioka, H.; Matsuoka, K.; Moroi, Y. Temperature Effect on Formation of Sodium Cholate Micelles. *J. Colloid Interface Sci.* **2003**, *259*, 156−162.

(12) Coello, A.; Meijide, F.; Rodríguez, N. E.; Tato, V. J. Aggregation Behavior of Bile Salts in Aqueous Solution. *J. Pharm. Sci.* **1996**, *85*, 9−15.

(13) Garidel, P.; Hildebrand, A.; Neubert, R.; Blume, A. Thermodynamic Characterization of Bile Salt Aggregation as a Function of Temperature and Ionic Strength Using Isothermal Titration Calorimetry. *Langmuir* **2000**, *16*, 5267−5275.

(14) Lindman, B.; Kamenka, N.; Fabre, H.; Ulmius, J.; Wieloch, T. Aggregation, Aggregate Composition, and Dynamics in Aqueous Sodium Cholate Solutions. *J. Colloid Interface Sci.* **1980**, *73*, 556−565.

(15) Partay, L. B.; Jedlovszky, P.; Sega, M. Molecular Aggregates in Aqueous Solutions of Bile Acid Salts. Molecular Dynamics Simulation Study. *J. Phys. Chem. B* **2007**, *111*, 9886−9896.

(16) Partay, L.; Sega, M.; Jedlovszky, P. Morphology of Bile Salt Micelles as Studied by Computer Simulation Methods. *Langmuir* **2007**, *23*, 12322−12328.

(17) Warren, D.; Chalmers, D. K.; Hutchison, K.; Dang, W.; Pouton, C. W. Molecular Dynamics Simulations of Spontaneous Bile Salt Aggregation. *Colloids Surf., A* **2006**, *280*, 182−193.

(18) Verde, A.; Frenkel, D. Simulation Study of Micelle Formation by Bile Salts. *Soft Matter* **2010**, *6*, 3815−3825.

(19) Vinarov, Z.; Petrova, L.; Tcholakova, S.; Denkov, N.; Stoyanov, S.; Lips, A. In Vitro Study of Triglyceride Lipolysis and Phase Distribution of the Reaction Products and Cholesterol: Effects of Calcium and Bicarbonate. *Food Funct.* **2012**, *3*, 1206−1220.

(20) Cornell, W. D.; Cieplak, P.; Bayly, C. I.; Gould, I. R.; Merz, K. M., Jr.; Ferguson, D. M.; Spellmeyer, D. C.; Fox, T.; Caldwell, J. W.; Kollman, P. A. A Second Generation Force Field for the Simulation of Proteins, Nucleic Acids, and Organic Molecules. *J. Am. Chem. Soc.* **1995**, *117*, 5179−5197.

(21) Wang, J.; Cieplak, P.; Kollman, P. A. How Well does a Restrained Electrostatic Potential (RESP) Model Perform in Calculating Conformational Energies of Organic and Biological Molecules? *J. Comput. Chem.* **2000**, *21*, 1049−1074.

(22) Jorgensen, W. L.; Chandrasekhar, J.; Madura, J. D.; Impey, R. W.; Klein, M. L. Comparison of Simple Potential Functions for Simulating Liquid Water. *J. Chem. Phys.* **1983**, *79*, 926−935.

(23) Wang, J. M.; Wolf, R. M.; Caldwell, J. W.; Kollman, P. A.; Case, D. A. Development and Testing of a General Amber Force Field. *J. Comput. Chem.* **2004**, *25*, 1157−1174.

(24) Bayly, C. I.; Cieplak, P.; Cornell, W. D.; Kollman, P. A. A Well Behaved Electrostatic Potential Based Method Uusing Charge Restraints for Deriving Atomic Charges − the RESP Model. *J. Phys. Chem.* **1993**, *97*, 10269−10280.

(25) Cieplak, P.; Cornell, W. D.; Bayly, C.; Kollman, P. A. Application of the Multimolecule and Multiconformational RESP Methodology to Biopolymers − Charge Derivation for DNA, RNA, and Proteins. *J. Comput. Chem.* **1995**, *16*, 1357−1377.

(26) Becke, A. D. Density-functional Exchange-energy Approximation with Correct Asymptotic Behavior. *Phys. Rev. A: At., Mol., Opt. Phys.* **1988**, *38*, 3098−3100.

(27) Becke, A. D. Density-functional Thermochemistry. III. The role of Exact Exchange. *J. Chem. Phys.* **1993**, *98*, 5648−5652.

(28) Lee, C.; Yang, W.; Parr, R. G. Development of the Colle-Salvetti Correlation-energy Formula into a Functional of the Electron Density. *Phys. Rev. B: Condens. Matter Mater. Phys.* **1988**, *37*, 785−789.

(29) Miehlich, B.; Savin, A.; Stoll, H.; Preuss, H. Results Obtained with the Correlation Energy Density Functionals of Becke and Lee, Yang and Parr. *Chem. Phys. Lett.* **1989**, *157*, 200−206.

(30) Ditchfield, R.; Hehre, W. J.; Pople, J. A. Self-consistent Molecular-orbital Methods. IX. An Extended Gaussian-type Basis for Molecular-orbital Studies of Organic Molecules. *J. Chem. Phys.* **1971**, *54*, 724−728.




DOI: 10.1021/acs.jpcb.5b07063
*J. Phys. Chem. B* 2015, 119, 15631−15643

(31) Frisch, M. J.; Trucks, G. W.; Schlegel, H. B.; Scuseria, G. E.; Robb, M. A.; Cheeseman, J. R.; Scalmani, G.; Barone, V.; Mennucci, B.; Petersson, G. A.; et al. *Gaussian 09, Revision D.01*; Gaussian, Inc.: Wallingford, CT, 2009 (full citation is provided in the Supporting Information).
(32) Berendsen, H. J. C.; Postma, J. P. M.; DiNola, A.; Haak, J. R.; van Gunsteren, W. F. Molecular Dynamics with Coupling to an External Bath. *J. Chem. Phys.* **1984**, *81*, 3684−3691.
(33) Miyamoto, S.; Kollman, P. A. Settle: An analytical Version of the SHAKE and RATTLE Algorithm for Rigid Water Models. *J. Comput. Chem.* **1992**, *13*, 952−962.
(34) Ryckaert, J.-P.; Ciccotti, G.; Berendsen, H. J. C. Numerical Integration of the Cartesian Equations of Motion of a System with Constraints: Molecular Dynamics of n-Alkanes. *J. Comput. Phys.* **1977**, *23*, 327−341.
(35) Darden, T.; York, D.; Pedersen, L. Particle Mesh Ewald: An N·log(N) Method for Ewald Sums in Large Systems. *J. Chem. Phys.* **1993**, *98*, 10089−10092.
(36) Essmann, U.; Perera, L.; Berkowitz, M. L.; Darden, T.; Lee, H.; Pedersen, L. G. A Smooth Particle Mesh Ewald Method. *J. Chem. Phys.* **1995**, *103*, 8577−8593.
(37) Toukmaji, A.; Sagui, C.; Board, J.; Darden, T. Efficient PME-based Approach to Fixed and Induced Dipolar Interactions. *J. Chem. Phys.* **2000**, *113*, 10913−10927.
(38) van der Spoel, D.; Lindahl, E.; Hess, B.; Groenhof, G.; Mark, A. E.; Berendsen, H. J. C. GROMACS: Fast, Flexible, and Free. *J. Comput. Chem.* **2005**, *26*, 1701−1718.
(39) Humphrey, W.; Dalke, A.; Schulten, K. VMD: Visual Molecular Dynamics. *J. Mol. Graphics* **1996**, *14*, 33−38.
(40) Korsunskiy, V. I.; Neder, R. B. Exact Model Calculations of the Total Radial Distribution Functions for the X-ray Diffraction Case and Systems of Complicated Chemical Composition. *J. Appl. Crystallogr.* **2005**, *38*, 1020−1027.
(41) Madenci, D.; Egelhaaf, S. U. Self-assembly in Aqueous Bile Salt Solutions. *Curr. Opin. Colloid Interface Sci.* **2010**, *15*, 109−115.
(42) Abel, S.; Dupradeau, F.-Y.; Marchi, M. Molecular Dynamics Simulations of a Characteristic DPC Micelle in Water. *J. Chem. Theory Comput.* **2012**, *8*, 4610−4623.
(43) Arunan, E.; Desiraju, G. R.; Klein, R. A.; Sadlej, J.; Scheiner, S.; Alkorta, I.; Clary, D. C.; Crabtree, R. H.; Dannenberg, J. J.; Hobza, P.; et al. Definition of the Hydrogen Bond (IUPAC Recommendations 2011). *Pure Appl. Chem.* **2011**, *83*, 1637−1641 (full citation is provided in the Supporting Information).
(44) Israelachvili, J. N. *Intermolecular and Surface Forces*; Academic Press: New York, 1992.


DOI: 10.1021/acs.jpcb.5b07063
*J. Phys. Chem. B* 2015, 119, 15631−15643